

RESEARCH OUTPUTS / RÉSULTATS DE RECHERCHE

Bounds on ortho-positronium and J/ψ - Υ quarkonia invisible decays and constraints on hidden braneworlds in a $SO(3,1)$ -broken 5D bulk

Sarrazin, Michaël; Stasser, Coraline

Published in:
International Journal of Modern Physics A

Publication date:
2020

Document Version
Peer reviewed version

[Link to publication](#)

Citation for pulished version (HARVARD):
Sarrazin, M & Stasser, C 2020, 'Bounds on ortho-positronium and J/ψ - Υ quarkonia invisible decays and constraints on hidden braneworlds in a $SO(3,1)$ -broken 5D bulk', *International Journal of Modern Physics A*, vol. 35, no. 2050032.

General rights

Copyright and moral rights for the publications made accessible in the public portal are retained by the authors and/or other copyright owners and it is a condition of accessing publications that users recognise and abide by the legal requirements associated with these rights.

- Users may download and print one copy of any publication from the public portal for the purpose of private study or research.
- You may not further distribute the material or use it for any profit-making activity or commercial gain
- You may freely distribute the URL identifying the publication in the public portal ?

Take down policy

If you believe that this document breaches copyright please contact us providing details, and we will remove access to the work immediately and investigate your claim.

Bounds on ortho-positronium and $J/\psi - \Upsilon$ quarkonia invisible decays and constraints on hidden braneworlds in a $SO(3,1)$ -broken 5D bulk

Michaël Sarrazin^{1,2,*} and Coraline Stasser²

¹*Institut UTINAM, CNRS/INSU, UMR 6213, Université Bourgogne-Franche-Comté,
16 route de Gray, F-25030 Besançon Cedex, France*

²*Laboratory of Analysis by Nuclear Reactions, Department of Physics,
University of Namur, 61 rue de Bruxelles, B-5000 Namur, Belgium*

While our visible Universe could be a 3-brane, some cosmological scenarios consider that other 3-branes could be hidden in the extra-dimensional bulk. Matter disappearance toward a hidden brane is mainly discussed for neutron – both theoretically and experimentally – but other particles are poorly studied. Recent experimental results offer new constraints on positronium or quarkonium invisible decays. In the present work, we show how a two-brane Universe allows for such invisible decays. We put this result in the context of the recent experimental data to constrain the brane energy scale M_B (or effective brane thickness M_B^{-1}) and the interbrane distance d for a relevant two-brane Universe in a $SO(3,1)$ -broken 5D bulk. Quarkonia present poor bounds compared to results deduced from previous passing-through-walls-neutron experiments for which scenarios with $M_B < 2.5 \times 10^{17}$ GeV and $d > 0.5$ fm are excluded. By contrast, positronium experiments can compete with neutron experiments depending on the matter content of each brane. To constrain scenarios up to the Planck scale, positronium experiments in vacuum cavity should be able to reach $\text{Br}(\text{o-Ps} \rightarrow \text{invisible}) \approx 10^{-6}$.

PACS numbers: 11.25.Wx, 36.10.Dr, 13.20.Gd

Many cosmological scenarios consider the existence of hidden braneworlds, specifically to explain the origin of dark matter and dark energy or as alternatives to cosmic inflation [1–11]. Among the cosmological models of interest, universes involving $SO(3,1)$ -broken 5D bulks containing at least two braneworlds are under consideration [8–10]. In the last decade, it has been shown that such scenarios imply matter exchange between branes, which is a possible way to test these models [12–17]. In this context, neutron disappearance (reappearance) toward (from) a hidden brane has been widely discussed both theoretically [12–14] and experimentally [15–17]. Nevertheless, other kinds of particles have been somewhat neglected, although with good reason. In the present paper, we consider recent experimental results about constraints on positronium [18, 19] or quarkonium [20] invisible decays in vacuum¹. These works [18, 19] were themselves

motivated by the possibility of invisible decays along extra dimensions [23], a situation somewhat similar but different from the present one involving hidden braneworlds. Here, showing how a hidden braneworld allows for such invisible decays, we discuss about constraints on the distance between our visible brane and a hidden one, and on the brane energy scale (or brane thickness) in the bulk. Highlighting the significant efficiency of the neutron to probe the existence of hidden braneworld, we put theoretical constraints on the expected branching ratio for positronium and quarkonium invisible decays.

When considering a two-brane Universe, whatever its full high-energy description (i.e. whatever the number or properties of bulk scalar fields responsible for particle trapping on branes, the number of extra dimensions or the bulk metric, etc.), the fermion dynamics on both branes at a sub-GeV energy scale is the same as the dynamics of fermions in a $M_4 \times Z_2$ space-time in the context of the non-commutative geometry [12, 13]. There are then two copies of the Standard Model, each sector being localized in each brane. Assuming that each braneworld is a M_B^{-1} -thick domain wall – where M_B is the brane energy scale – the two sectors are mutually invisible to each other at the zeroth-order approximation for processes with energies below M_B . By contrast, matter fields in separate branes can mix at a first-order approximation mainly through the Lagrangian $\mathcal{L}_c = ig\bar{\psi}_+\gamma^5\psi_- + ig\bar{\psi}_-\gamma^5\psi_+$, where ψ_{\pm} are the Dirac

*Electronic address: michael.sarrazin@ac-besancon.fr; Corresponding author

¹ In a previous work [21], the constraint on $\text{Br}(\text{o-Ps} \rightarrow \text{invisible})$ is stronger by 3 orders of magnitude when compared to the work here under consideration [18]. However, this constraint [21] is obtained from measurements performed in presence of matter such that o-Ps undergoes very high collision rates [18, 21]. Then, decay rate calculation requires extrapolations [18, 21, 22], to account of collisions consequences, leading to large uncertainties [18, 21]. As a result, there is a need for experiments with low collision rates – or in vacuum – to avoid any extrapolation [18]. Nevertheless, uncertainties could be restrained thanks to complex GEANT4 simulations possibly supplemented with a density matrix approach, as done for neutron-hidden neutron dynamics in nuclear reactors [15, 16], for instance. This significant further work is far beyond the topic of the present work aiming to demonstrate the relevance of positronium experiments to track

hidden braneworlds. Thus, for now, we chose to consider the conservative but robust constraint from experiments in vacuum cavity only [18].

fermionic fields in each braneworld – denoted (+) and (–) [12, 13]. The interbrane coupling g is given by [12]:

$$g = (m^2/M_B) \exp(-md), \quad (1)$$

and depends on the distance d between branes, on their effective thickness M_B^{-1} and on the mass m of the particle of the Standard Model under consideration, i.e. a constituent quark [12, 24–27] or a lepton. More specifically for bound quarks, g presents a cut-off at $d \approx 0.5$ fm beyond which it cancels [12].

From \mathcal{L}_c one can show that a particle could oscillate between two states, one localized in our brane, the other localized in the hidden world. In fact, the oscillation would be driven by the effective magnetic field $\mathbf{B}_\perp = g(\mathbf{A}_+ - \mathbf{A}_-)$ transverse-like to the branes, where \mathbf{A}_\pm are the magnetic vector potentials in each brane. Specifically, the interaction Hamiltonian \mathbf{H}_c between the Pauli spinors of the visible and hidden worlds is given by [12–14]:

$$\mathbf{H}_c = \hbar\Omega \begin{pmatrix} 0 & \varepsilon \\ \varepsilon^\dagger & 0 \end{pmatrix}, \quad (2)$$

where $\varepsilon = -i\sigma \cdot \mathbf{B}_\perp/B_\perp = -i\sigma \cdot \mathbf{n}$ is a unitary matrix acting on the spin with $\mathbf{n} = (\sin\theta \cos\varphi, \sin\theta \sin\varphi, \cos\theta)$, and $\hbar\Omega = \mu_n B_\perp$ with μ_n the magnetic moment of the particle. Here vector potentials \mathbf{A}_\pm are dominated by the huge ($\gtrsim 10^9$ T m) overall astrophysical magnetic vector potential \mathbf{A}_{amb} related to the magnetic fields of all the astrophysical objects (planets, stars, galaxies, etc.) [14, 15, 29–33] and such that $\mathbf{A}_+ - \mathbf{A}_- \approx \mathbf{A}_{amb}$ [14, 15].

In the present work we consider bound states $\bar{p}p$ constituted by a fermion p and its anti-particle \bar{p} . These states are characterized by a finite lifetime and some decay channels. More precisely, we consider the long-living 1^3S_1 state (ortho-state) and the short-living 1^1S_0 state (para-state) of the $p\bar{p}$ bound pair. Following the standard description, the ortho-state wave function can be expressed as [34]:

$$|\psi_1\rangle = |p, \uparrow\rangle \otimes |\bar{p}, \uparrow\rangle, \quad (3)$$

$$|\psi_{-1}\rangle = |p, \downarrow\rangle \otimes |\bar{p}, \downarrow\rangle, \quad (4)$$

$$|\psi_0\rangle = (1/\sqrt{2})(|p, \uparrow\rangle \otimes |\bar{p}, \downarrow\rangle + |p, \downarrow\rangle \otimes |\bar{p}, \uparrow\rangle), \quad (5)$$

and similarly for the para-state wave function, we have:

$$|\psi_P\rangle = (1/\sqrt{2})(|p, \uparrow\rangle \otimes |\bar{p}, \downarrow\rangle - |p, \downarrow\rangle \otimes |\bar{p}, \uparrow\rangle), \quad (6)$$

where $|p, \uparrow\rangle$ and $|\bar{p}, \uparrow\rangle$ relate to the wave functions of the fermion and its anti-particle respectively both taking into account the spin state.

Let us now consider the relevant interbrane coupling, which is simply the sum of two \mathbf{H}_c Hamiltonian operators corresponding to the contributions of the particle and its anti-particle [34]:

$$\mathbf{W} = -i\hbar\Omega \begin{pmatrix} 0 & (\sigma_p - \sigma_{\bar{p}}) \cdot \mathbf{n} \\ -(\sigma_p - \sigma_{\bar{p}}) \cdot \mathbf{n} & 0 \end{pmatrix}, \quad (7)$$

where the minus sign $(-\sigma_{\bar{p}})$ arises from the opposite magnetic moment of these particles. Considering the non-diagonal terms of the coupling term \mathbf{W} , and the $\bar{p}p$ wave functions, we get:

$$(\sigma_p - \sigma_{\bar{p}}) \cdot \mathbf{n} |\psi_1\rangle = -\sqrt{2}e^{i\varphi} \sin\theta |\psi_P\rangle, \quad (8)$$

$$(\sigma_p - \sigma_{\bar{p}}) \cdot \mathbf{n} |\psi_0\rangle = 2 \cos\theta |\psi_P\rangle, \quad (9)$$

$$(\sigma_p - \sigma_{\bar{p}}) \cdot \mathbf{n} |\psi_{-1}\rangle = \sqrt{2}e^{-i\varphi} \sin\theta |\psi_P\rangle, \quad (10)$$

$$\begin{aligned} & (\sigma_p - \sigma_{\bar{p}}) \cdot \mathbf{n} |\psi_P\rangle \\ &= 2 \cos\theta |\psi_0\rangle - \sqrt{2}e^{-i\varphi} \sin\theta |\psi_1\rangle + \sqrt{2}e^{i\varphi} \sin\theta |\psi_{-1}\rangle. \end{aligned} \quad (11)$$

It is noticeable that an ortho-state in a brane convert into a para-state only in the second brane and vice versa. Then, considering only the ortho-state in our brane², the relevant wave function to consider for matter exchange can be written as:

$$|\Psi\rangle = \begin{pmatrix} |\Psi_+\rangle \\ |\Psi_-\rangle \end{pmatrix} = \begin{pmatrix} |\Psi_O\rangle \\ |\Psi_P\rangle \end{pmatrix} = \begin{pmatrix} |\psi_1\rangle \\ |\psi_0\rangle \\ |\psi_{-1}\rangle \\ |\psi_P\rangle \end{pmatrix}, \quad (12)$$

where $|\Psi_\pm\rangle$ are the wave functions in each brane (+) or (–), and $|\Psi_{O/P}\rangle$ the wave functions for the ortho-state and para-state. The two-brane wave function $|\Psi(t)\rangle$ then follows:

$$i\hbar\partial_t |\Psi(t)\rangle = (\mathbf{H}_0 + \mathbf{W}) |\Psi(t)\rangle, \quad (13)$$

where the Hamiltonian \mathbf{W} can be recast as:

$$\mathbf{W} = \hbar\Omega \begin{pmatrix} \mathbf{0} & |\mathbf{C}\rangle \\ \langle\mathbf{C}| & \mathbf{0} \end{pmatrix} \text{ where } |\mathbf{C}\rangle = \begin{pmatrix} i\sqrt{2}e^{i\varphi} \sin\theta \\ -2i \cos\theta \\ -i\sqrt{2}e^{-i\varphi} \sin\theta \end{pmatrix}, \quad (14)$$

and where $\mathbf{H}_0 = \text{diag}(E_O - i\hbar\Gamma_O, E_O - i\hbar\Gamma_O, E_O - i\hbar\Gamma_O, E_P - i\hbar\Gamma_P)$. E_O (respectively E_P) is the eigenenergy and Γ_O (respectively Γ_P) is the decay rate of the ortho-state (respectively of the para-state).

$|\Psi(t)\rangle$ is obtained from the Lippmann–Schwinger equation:

$$|\Psi(t)\rangle = |\Psi^{(0)}(t)\rangle + \int_{-\infty}^{+\infty} G^{(0)}(t-t') \mathbf{W} |\Psi(t')\rangle dt', \quad (15)$$

² As shown in the following, the branching ratio of invisible decays of ortho-states is larger by many orders of magnitude by contrast to this of para-states.

$p\bar{p}$	state	Mass	Full width 2Γ	$\text{Br}(\text{o-}p\bar{p} \rightarrow \text{invisible})$
Positronium	o-Ps	$1.022 - \varepsilon$ MeV	$7.211 \times 10^6 \text{ s}^{-1}$ (th)	$< 5.9 \times 10^{-4}$ at 90 % C.L.
	p-Ps	$1.022 - \varepsilon'$ MeV	$8.033 \times 10^9 \text{ s}^{-1}$ (th)	-
Charmonium	J/ψ	3096.900 ± 0.006 MeV	92.9 ± 2.8 keV (exp)	$< 7 \times 10^{-4}$ at 90 % C.L.
	η_c	2983.4 ± 0.5 MeV	31.8 ± 0.8 MeV (exp)	-
Bottonium	Υ	9460.30 ± 0.26 MeV	54.02 ± 1.25 keV (exp)	$< 3.0 \times 10^{-4}$ at 90 % C.L.
	η_b	9399.0 ± 2.3 MeV	10^{+5}_{-4} MeV (exp)	-

TABLE I: Summary of positronium and quarkonium masses, full widths and invisible decay branching ratios from theoretical and experimental data [18, 20, 24–28]. ε and ε' describe the mass difference between the ortho-state and the para-state of the positronium, such that $|\varepsilon - \varepsilon'| = 0.84$ MeV.

where the propagator follows $(i\hbar\partial_t - \mathbf{H}_0)G^{(0)}(t - t') = \mathbf{1}\delta(t - t')$ such that $G^{(0)}(t - t') = -i\hbar^{-1}e^{-i\hbar^{-1}\mathbf{H}_0(t-t')}\Theta(t - t')$, with $\Theta(t)$ the Heaviside step function. $|\Psi^{(0)}(t)\rangle = i\hbar G^{(0)}(t)|\Psi^{(0)}\rangle$ is the solution of Eq. 13 when $\mathbf{W} = 0$ with

$$|\Psi^{(0)}\rangle = \begin{pmatrix} |\Psi_O^{(0)}\rangle \\ 0 \end{pmatrix} \text{ where } |\Psi_O^{(0)}\rangle = \begin{pmatrix} p \\ q \\ r \end{pmatrix}, \quad (16)$$

with $|p|^2 + |q|^2 + |r|^2 = 1$. $|\Psi^{(0)}\rangle$ defines the initial state when the particle is created. Assuming that $\hbar\Omega \ll E_O, E_P$ we use an up to the second-order expansion of the Lippmann–Schwinger equation such that:

$$|\Psi(t)\rangle \sim |\Psi^{(0)}(t)\rangle \quad (17)$$

$$+ \int_{-\infty}^{+\infty} G^{(0)}(t - t')\mathbf{W}|\Psi^{(0)}(t')\rangle dt' \\ + \int_{-\infty}^{+\infty} \int_{-\infty}^{+\infty} G^{(0)}(t - t')\mathbf{W}G^{(0)}(t' - t'')\mathbf{W}|\Psi^{(0)}(t'')\rangle dt'' dt'.$$

We are now going to calculate the whole decay rate Γ of the $\bar{p}p$ bound state in the two-brane Universe. We set $\Gamma = (1/2)\tau^{-1}$ where τ is the mean lifetime of the $\bar{p}p$ state given by $\tau = \int_0^\infty tf(t)dt$ where the related distribution function for the probability to observe the particle is $f(t) = -(d/dt)P$ with $P = \langle\Psi(t)|\Psi(t)\rangle$. Then, we get: $\Gamma^{-1} = 2 \int_0^\infty \langle\Psi(t)|\Psi(t)\rangle dt$. Using Eq. 17, we can now express $\langle\Psi(t)|\Psi(t)\rangle$ up to the second order of approximation and we can simply compute Γ^{-1} :

$$\Gamma^{-1} \sim \frac{1}{\Gamma_O} + \frac{\Gamma_O^2 - \Gamma_P^2}{\Gamma_P\Gamma_O^2} \left| \langle\mathbf{C}|\Psi_O^{(0)}\rangle \right|^2 \quad (18) \\ \times \frac{\Omega^2}{\hbar^{-2}(E_O - E_P)^2 + (\Gamma_O + \Gamma_P)^2},$$

where $\left| \langle\mathbf{C}|\Psi_O^{(0)}\rangle \right|^2 = |\sqrt{2}(e^{i\varphi}r - e^{-i\varphi}p)\sin\theta + 2q\cos\theta|^2$.

It is noticeable that the result depends on the polarization state of the ortho-state compared with the direction \mathbf{n} of the effective magnetic field $\mathbf{B}_\perp = \mathbf{n}B_\perp$ while it is not the case for a neutron for instance [14]³. Anyway, in most experiments, there is no way for the particles to be produced with a fixed polarization. In this case, $\left| \langle\mathbf{C}|\Psi_O^{(0)}\rangle \right|^2 = 4/3$ for unpolarized particles. From Eq. 18 we can deduce the whole decay rate Γ :

$$\Gamma = \Gamma(\text{o-}p\bar{p} \rightarrow \text{visible decay}) + \Gamma(\text{o-}p\bar{p} \rightarrow \text{invisible}), \quad (19)$$

with

$$\Gamma(\text{o-}p\bar{p} \rightarrow \text{visible decay}) = \Gamma_O \left(1 - \frac{\Gamma_O}{\Gamma_P} \mathcal{R} \right), \quad (20)$$

and

$$\Gamma(\text{o-}p\bar{p} \rightarrow \text{invisible}) = \Gamma_P \mathcal{R}, \quad (21)$$

and where

$$\mathcal{R} = \left| \langle\mathbf{C}|\Psi_O^{(0)}\rangle \right|^2 \frac{\Omega^2}{\hbar^{-2}(E_O - E_P)^2 + (\Gamma_O + \Gamma_P)^2}. \quad (22)$$

Thus, the invisible decay rate (see Eq. 21) is simply the para-state decay rate (since o- $p\bar{p}$ converts into p- $p\bar{p}$ in the hidden brane) weighted by \mathcal{R} , the probability of swapping from our visible braneworld to the hidden brane.

³ For a neutron with a given polarization state such that $|u\rangle = \alpha|\uparrow\rangle + \beta|\downarrow\rangle$ (with $|\alpha|^2 + |\beta|^2 = 1$), considering the off-diagonal terms of \mathbf{H}_c proportional to $\sigma \cdot \mathbf{n}$, we get $\sigma \cdot \mathbf{n}|u\rangle = \alpha'|\uparrow\rangle + \beta'|\downarrow\rangle$. Although $(\alpha', \beta') \neq (\alpha, \beta)$ in most cases (i.e. the polarization is modified when the neutron leaps into the hidden brane), one gets: $|\alpha'|^2 + |\beta'|^2 = 1$ such that the swapping amplitude does not depend on the polarization state of the neutron. It is not longer the case of the $p\bar{p}$ states here under consideration due to the structure of their wave functions.

By contrast, Eq. 20 shows that $o\text{-}p\bar{p}$ decay products – recorded in our visible world – must occur at a lower rate since some particles are lost through decays in the hidden brane. At last, Eq. 21 shows that some decays must occur as invisible ones leading to an apparent loss of energy which is more easily detectable than a change of the visible $o\text{-}p\bar{p}$ decay rate.

Finally, we simply deduce the branching ratio for the invisible decay of unpolarized particles:

$$\text{Br}(o\text{-}p\bar{p} \rightarrow \text{invisible}) = \frac{4}{3} \frac{\Gamma_P}{\Gamma_O} \times \frac{\Omega^2}{\hbar^{-2} (E_O - E_P)^2 + (\Gamma_O + \Gamma_P)^2} \quad (23)$$

As a remark, similar calculations can be done in order to obtain the branching ratio $\text{Br}(p\text{-}p\bar{p} \rightarrow \text{invisible})$ for the invisible decay of para-states. As a result, one then gets:

$$\frac{\text{Br}(p\text{-}p\bar{p} \rightarrow \text{invisible})}{\text{Br}(o\text{-}p\bar{p} \rightarrow \text{invisible})} = 3 \left(\frac{\Gamma_O}{\Gamma_P} \right)^2, \quad (24)$$

such that $\text{Br}(p\text{-}p\bar{p} \rightarrow \text{invisible})$ is up to 6 (respectively 5 and 4) orders of magnitude smaller than $\text{Br}(o\text{-}p\bar{p} \rightarrow \text{invisible})$ for positronium (respectively charmonium and bottomonium), thus justifying to focus only on invisible decays of ortho-states.

We are now investigating the ortho-positronium ($o\text{-Ps}$) (respectively the J/ψ charmonium and the Υ bottomonium) invisible decay through its conversion into para-positronium ($p\text{-Ps}$) (respectively η_c charmonium and η_b bottomonium) in the hidden brane.

Equation 23 applies by using the relevant parameters (see table I). Here the difference $E_O - E_P$ includes the following contributions:

$$E_O - E_P = (m_O - m_P) c^2 + m_O V_+ - m_P V_- \quad (25)$$

where m_O and m_P are the masses of the ortho-state and of the para-state respectively, and V_{\pm} are the gravitational potentials in each brane. Doing this, we consider the following hypotheses:

(i) *Null electric dipole moment hypothesis*

In our previous works [12, 16, 17], it has been underlined that the interaction between the magnetic vector potential and the charge of a particle precludes the particle swapping between branes. As a consequence, since we consider electron/positon pairs or quark/antiquark pairs, we must consider these pairs as strictly chargeless and without charge structure. Let E_{bind} be the typical binding energy of the fermion/antifermion pair. Then, the time $\Delta t \sim \hbar/E_{bind}$ during which quantum fluctuations allow for an instantaneous electric dipole moment (EDM) must be smaller than the period $T \sim \hbar/(E_O - E_P)$ of the Rabi oscillation during which the $p\bar{p}$ state oscillates between each brane. This allows a time averaged EDM equal to zero. That means that $E_O - E_P \ll E_{bind}$ must be verified. This condition is

verified in quarkonium where the mass-energy difference between the ortho and para states dominates (i.e. $E_O - E_P \sim (m_O - m_P) c^2$). Indeed, $E_{bind} \approx 1$ GeV and ≈ 0.7 GeV while $E_O - E_P \approx 61$ MeV and ≈ 114 MeV for the bottomonium and the charmonium respectively [28]. By contrast, for the positronium the gravitational potential is now dominant (i.e. $E_O - E_P \sim m_{Ps} (V_+ - V_-)$) and $E_{bind} \approx 6.8$ eV [34]. Then, positronium is a relevant probe if $|V_+ - V_-| \lesssim 10^{-6} c^2$. The consequence of this is discussed later in this paper.

$p\bar{p}$	$\hbar\Omega$	p (or \bar{p})	g
$o\text{-Ps}$	$< 6.4 \times 10^{-4}$ eV	e^-/e^+	$< 1.1 \times 10^{-8}$ m $^{-1}$
J/ψ	< 0.15 MeV	c/\bar{c}	$< 1.2 \times 10^4$ m $^{-1}$
Υ	< 0.10 MeV	b/\bar{b}	$< 4.8 \times 10^4$ m $^{-1}$
n (udd)	< 0.14 eV	u or d	$< 2.4 \times 10^{-3}$ m $^{-1}$

TABLE II: Derived constraints on $\hbar\Omega$ for positronium and quarkonium, and on the interbrane coupling constant g for some Standard Model particles. The quark constituent masses used are $m_b = 4730$ MeV and $m_c = 1550$ MeV [24–28]. Neutron results are derived from previous experimental results [15] and given for comparison.

(ii) *Global gravitational potential hypothesis*

The gravitational potential V_{\pm} felt by the particles incorporates many contributions. Some are local and others are more global at a cosmological scale. Matter distribution can be considered as homogeneous and isotropic at a cosmological scale. If the second brane is similar to our own, then the difference of the gravitational contributions of each brane vanishes when considering large scale contributions only. As a consequence, the difference of the gravitational contributions of each brane just depends on fluctuations of local mass distributions in each brane at various scales. The first contribution comes from matter fluctuations related to large-scale galactic superstructures [35, 36]. The amplitude of such fluctuations is characterized by the well-known parameter σ_8 [35, 36], which allows to estimate the amplitude V_C of the gravitational potential at the level of large-scale superstructures [36]. Here we get [36]: $V_C = (3/2)\Omega_{m0} (8 \text{ Mpc}/H_0^{-1})^2 \sigma_8 \approx 10^{-5} c^2$ (where Ω_{m0} is the present-day density parameter for baryons and cold dark matter, and H_0 the Hubble constant). At a closer scale, Milky Way contributes for $V_{MW} \approx 5 \times 10^{-7} c^2$, while the Sun, the Earth, and the Moon provide lower contributions of about $10^{-8} c^2$, $7 \times 10^{-10} c^2$, and $10^{-13} c^2$, respectively [14]. Considering hidden branes similar to our own, or with a lower matter content, V_C should allow to define an upper constraint on $|V_+ - V_-| < 10^{-5} c^2$.

(iii) *Global magnetic vector potential hypothesis*

The overall ambient astrophysical magnetic vector

potential \mathbf{A}_{amb} was previously discussed in the literature in a different context [29–33]. \mathbf{A}_{amb} is the sum of all of the magnetic vector potential contributions related to the magnetic fields of astrophysical objects (planets, stars, galaxies, etc.) since $\mathbf{B}(\mathbf{r}) = \nabla \times \mathbf{A}(\mathbf{r})$. At large distances from sources (for instance, close to the Earth), \mathbf{A}_{amb} is almost uniform (i.e. $\nabla \times \mathbf{A}_{amb} \approx \mathbf{0}$) and cannot be cancelled out with magnetic shields [33]. As a rule of thumb, $A \approx DB$ where D is the distance from the astrophysical source and B is the typical field induced by the object. The expected order of magnitude of A_{amb} can be then roughly constrained. Galactic magnetic field variations on local scales towards the Milky Way core ($A_{amb} \approx 2 \times 10^9$ T m) are usually assumed [29–33]. By contrast, the Earth’s magnetic field leads to 200 T m while the Sun contributes 10 T m [33]. By contrast, the magnitude of intergalactic contributions are less clear [14]). Then, for now A_{amb} can be fairly bounded by the lower estimated value: $A_{amb} = 10^9$ T m.

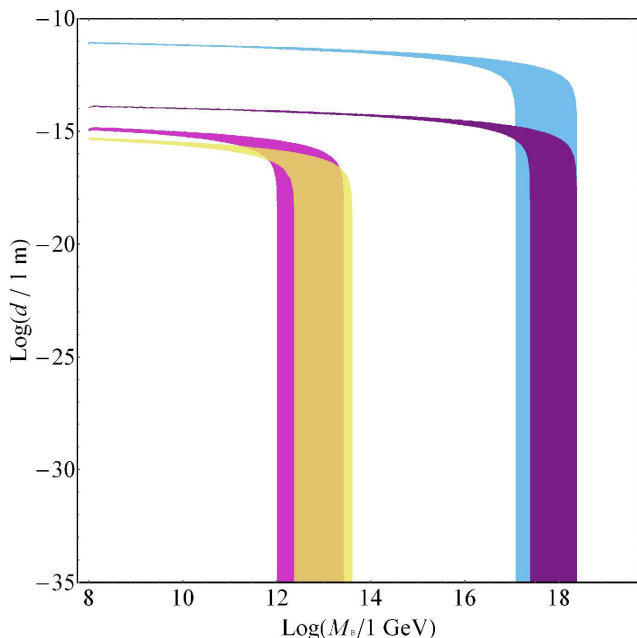


FIG. 1: (Color online). Bounds on the brane energy scale M_B and on the interbrane distance d derived from each particle kind: bottomonium (yellow), charmonium (magenta), positronium (cyan) and neutron (purple). Each domain on the left of a colored band is excluded. Each colored band widens to the right when sensitivity increases: up to the Planck scale for neutron and positronium ($\text{Br}(\text{o-Ps} \rightarrow \text{invisible}) = 1.4 \times 10^{-6}$), up to $\text{Br}(\text{quarkonium} \rightarrow \text{invisible}) = 10^{-6}$ for quarkonia.

As a result, from table I and Eq. 23 we deduce the results shown in table II. Table II gives the upper bounds for the coupling constants ($\hbar\Omega$ or g) both for bound states and some fundamental particles of the Standard Model. From table II data and Eq. 1, we can now derive lower bounds on the brane energy scale M_B and upper bounds on the interbrane distance d – for a $SO(3,1)$ -

broken $M_4 \times R_1$ bulk – which are independent of the particle under consideration. The results are summarized on Fig. 1. Each domain on the left of a colored band is excluded: If matter disappearance can occur in the present braneworld scenario, these values of (M_B, d) are not relevant. One notes that bounds are much poorer for quarkonia than for positronium or neutron. For the latter, it is noticeable that the constraints are just one order of magnitude below the reduced Planck energy scale, except if one accepts as possible a fine tuning of the distance d between 1 fm or 1 Å allowing for significantly low values for M_B (see Fig. 1). To be more quantitative, table III (left column) gives the bounds of the brane energy scale M_B for each particle.

Particle	M_B	$\text{Br}(\text{o-}p\bar{p} \rightarrow \text{invisible})$
o-Ps	$> 1.2 \times 10^{17}$ GeV	1.4×10^{-6}
J/ψ	$> 1.0 \times 10^{12}$ GeV	1.3×10^{-16}
Υ	$> 2.4 \times 10^{12}$ GeV	2.9×10^{-16}
neutron	$> 2.5 \times 10^{17}$ GeV	

TABLE III: Left column: Various bounds on the brane energy scale M_B derived from each particle kind for interbrane distances below 0.5 fm. Right column: Expected branching ratios for a brane energy scale at the reduced Planck energy (2.43×10^{18} GeV).

Considering the same two-brane scenario and assuming now that the brane energy scale is the reduced Planck energy scale, we can derive the expected branching ratio for the positronium and quarkonia invisible decays (see right column in table III), which need to be reached to observe the phenomenon. While the expected branching ratio for quarkonia is far beyond any current experimental skill, it is not the case for positronium which could compete with neutron to constrain braneworld scenarios [15–17]. In addition, in Fig. 1, each colored band widens to the right when sensitivity increases: up to the Planck scale for neutron and positronium ($\text{Br}(\text{o-Ps} \rightarrow \text{invisible}) = 1.4 \times 10^{-6}$), up to $\text{Br}(\text{quarkonium} \rightarrow \text{invisible}) = 10^{-6}$ for quarkonia.

As a major result, pretty low-energy experiments – involving positronium or neutron – appear then more suitable to probe the Planck scale than experiments needing colliders to produce quarkonia states. Even for a brane energy scale M_B at the Planck energy, low-energy disappearance phenomena can occur and could be observed in future low-energy experiments while the Planck scale is directly unreachable with colliders. However, to occur, positronium oscillations imply that the gravitational potentials in each brane must verify $|V_+ - V_-| \lesssim 10^{-6}c^2$, i.e. a value one order of magnitude lower than the upper gravitational constraint mentioned above. As a result, positronium and neutron experiments are complementary as they could allow to discriminate between two kinds of gravitational environment.

Acknowledgements

C.S. is supported by a FRiA doctoral grant from the Belgian F.R.S-FNRS. The authors thank Nicolas

Reckinger for reading the manuscript.

-
- [1] D. Battefeld, P. Peter, Phys. Rept. **571** (2015) 1, arXiv:1406.2790 [astro-ph.CO].
 - [2] T. Koivisto, D. Wills, I. Zavala, JCAP **06** (2014) 036, arXiv:1312.2597 [hep-th].
 - [3] R. Maartens, K. Koyama, Living Rev. Relativity **13** (2010) 5, arXiv:1004.3962 [hep-th].
 - [4] J.-L. Lehnert, Phys. Rept. **465** (2008) 223, arXiv:0806.1245 [astro-ph].
 - [5] P. Brax, C. van de Bruck, A.-C. Davis, Rep. Prog. Phys. **67** (2004) 2183, arXiv:hep-th/0404011.
 - [6] J. Khoury, B.A. Ovrut, P.J. Steinhardt, N. Turok, Phys. Rev. D **64** (2001) 123522, arXiv:hep-th/0103239.
 - [7] N. Arkani-Hamed, S. Dimopoulos, G. Dvali, N. Kaloper, JHEP **0012** (2000) 010, arXiv:hep-ph/9911386.
 - [8] D.J.H. Chung, K. Freese, Phys. Rev. D **67** (2003) 103505, arXiv:astro-ph/0202066.
 - [9] D.J.H. Chung, E.W. Kolb, A. Riotto, Phys. Rev. D **65** (2002) 083516, arXiv:hep-ph/0008126.
 - [10] D.J.H. Chung, K. Freese, Phys. Rev. D **62** (2000) 063513, arXiv:hep-ph/9910235.
 - [11] L. Visinelli, N. Bolis, S. Vagnozzi, Phys. Rev. D **97** (2018) 064039, arXiv:1711.06628 [gr-qc].
 - [12] C. Stasser, M. Sarrazin, Int. J. Mod. Phys. A **34** (2019) 1950029, arXiv:1612.02225 [hep-ph].
 - [13] M. Sarrazin, F. Petit, Phys. Rev. D **81** (2010) 035014, arXiv:0903.2498 [hep-th].
 - [14] M. Sarrazin, F. Petit, Eur. Phys. J. C **72** (2012) 2230, arXiv:1208.2014 [hep-ph].
 - [15] M. Sarrazin, et al., Phys. Lett. B **758** (2016) 14, arXiv:1604.07861 [hep-ex].
 - [16] M. Sarrazin, et al., Phys. Rev. D **91** (2015) 075013, arXiv:1501.06468 [hep-ph].
 - [17] M. Sarrazin, G. Pignol, F. Petit, V.V. Nesvizhevsky, Phys. Lett. B **712** (2012) 213, arXiv:1201.3949 [hep-ph].
 - [18] C. Vigo, L. Gerchow, L. Liskay, A. Rubbia, P. Crivelli, Phys. Rev. D **97** (2018) 092008, arXiv:1803.05744 [hep-ex].
 - [19] S.N. Gninenko, Phys. Rev. D **91** (2015) 015004, arXiv:1409.2288 [hep-ph].
 - [20] C. Patrignani *et al* (Particle Data Group), Chin. Phys. C **40** (2016) 100001.
 - [21] A. Badertscher, P. Crivelli, W. Fetscher, U. Gendotti, S. Gninenko, V. Postoev, A. Rubbia, V. Samoylenko, D. Sillou, Phys. Rev. D **75** (2007) 032004, arXiv:hep-ex/0609059.
 - [22] R. Foot, S. N. Gninenko, Phys. Lett. B **480** (2000) 171, arXiv:hep-ph/0003278.
 - [23] S. N. Gninenko, N. V. Krasnikov, Phys. Rev. D **67** (2003) 075012, arXiv:hep-ph/0302205.
 - [24] D. Griffiths, *Introduction to Elementary Particles*, Wiley-VCH Verlag GmbH & Co. KGaA (2008).
 - [25] W. Lucha, F.F. Schöberl, D. Gromes, Phys. Rep. **200** (1991) 127.
 - [26] H.J. Lipkin, Phys. Lett. B **233** (1989) 446.
 - [27] I. Cohen, H.J. Lipkin, Phys. Lett. **93B** (1980) 56.
 - [28] H. Satz, J. Phys. G **32** (2006) R25, arXiv:hep-ph/0512217.
 - [29] D.D. Ryutov, Phys. Rev. Lett. **103** (2009) 201803.
 - [30] E. Adelberger, G. Dvali, A. Gruzinov, Phys. Rev. Lett. **98** (2007) 010402, arXiv:hep-ph/0306245.
 - [31] J. Luo, L.-C. Tu, Z.-K. Hu, E.-J. Luan, Phys. Rev. Lett. **90** (2003) 081801.
 - [32] J. Luo, C.-G. Shao, Z.-Z. Liu, Z.-K. Hu, Phys. Lett. A **270** (2000) 288.
 - [33] R. Lakes, Phys. Rev. Lett. **80** (1998) 1826.
 - [34] O. Halpern, Phys. Rev. **94** (1954) 904.
 - [35] P. Schneider, *Extragalactic Astronomy and Cosmology*, Springer (2015).
 - [36] P. Peter, J.-P. Uzan, *Primordial Cosmology*, Oxford Graduate Texts (2013).